Universitat Autònoma de Barcelona

Computational Analysis of Oxygen Transfer in a Gene Therapy Bioreactor Using CFD Simulation

Maria Dolores Gonzalez Corvillo

MÀSTER EN ENGINYERIA BIOLÒGICA I AMBIENTAL

TUTOR(S) DEL TFM Francesc Gòdia Casablanca
Laura Cervera Gracia

16/06/2025

Abstract

Advanced Therapy Medicinal Products (ATMPs), such as gene and cell therapies, require very tight control of bioreactor conditions. One of the biggest challenges when dealing with dense cell cultures is ensuring sufficient oxygen availability [1,2]. This project aimed to evaluate how aeration rate and agitation speed influence oxygen transfer efficiency in a 1-liter stirred bioreactor using Computational Fluid Dynamics (CFD), aiming to estimate the volumetric mass transfer coefficient (k_la) under different operating conditions.

A simplified bioreactor geometry was constructed in ANSYS Fluent 2025R1 (student version) [6], including a four-blade turbine impeller and a bottom sparger—aligned with real systems used in cell therapy labs [3]. Eight simulations were performed: four varying air-inlet velocity (0.01, 0.035, 0.06, 0.1 m/s) at constant agitation (50 rpm), and four varying stirring speed (50, 100, 200, 400 rpm) at fixed air velocity (0.01 m/s). The shared case (50 rpm, 0.01 m/s) served as a reference. We used an Euler–Euler multiphase model with species transport and Henry's law for mass transfer [4,5,6]. The model ran under isothermal conditions (energy equation automatically enabled).

Results showed DO levels peaked at 0.035 m/s aeration, while higher rpm led to reduced oxygen availability—likely due to bubble breakup from increased turbulence [5]. DO ranged from 1.18×10^{-5} to 6.33×10^{-5} kg/m³ across cases (note: ANSYS Fluent reports species concentrations in kg/m³; for reference, 1 mol/m³ ≈ 0.032 kg/m³ for O_2). These trends highlight how small changes critically affect oxygen transfer.

In summary, aeration and agitation both had significant impact, but higher rpm did not guarantee better oxygen transfer. Optimal setup was 0.035 m/s aeration with 50 rpm stirring. This demonstrates that CFD is a valuable tool for optimizing ATMP bioprocesses before experimental phases [2].

Summary

This Master's Thesis focuses on analysing oxygen transfer in a 1-liter stirred-tank bioreactor designed for cell culture in advanced therapies, using Computational Fluid Dynamics (CFD) simulations. Adequate oxygen supply is critical for maintaining cell viability in dense cultures, with k_la (volumetric oxygen mass transfer coefficient) being one of the key parameters for bioreactor design [1].

A simplified geometry of the bioreactor was created in ANSYS Fluent 2025R1, featuring a four-blade turbine impeller and a bottom sparger [5]. Eight simulations were carried out: four varying air inlet velocity (0.01–0.1 m/s) with constant agitation at 50 rpm, and four others varying agitation speed (50–400 rpm) with fixed aeration at 0.01 m/s. An Eulerian multiphase model was used, including species transport and mass transfer via Henry's law [3,4].

The results showed that moderate aeration (0.035 m/s) combined with low agitation (50 rpm) led to the highest dissolved oxygen (DO) concentrations. In contrast, increasing agitation caused a significant drop in DO, likely due to bubble fragmentation and reduced residence time in the transfer zone [2]. DO levels ranged from 1.18×10^{-5} to 6.33×10^{-5} kg/m³, highlighting how sensitive oxygen transfer is to process conditions.

Cross-sectional concentration profiles confirmed that high agitation caused peripheral oxygen accumulation and disrupted symmetrical gas dispersion. OTR and k_la values were calculated and matched the fluid dynamics and phase distribution patterns observed in the simulations.

Despite the use of a student version of Fluent and simplified models, the study shows how CFD can be a predictive tool to assess oxygenation strategies in early-stage ATMP process design. Further improvements may include finer spargers, in-line sensors, or experimental validation [2,5].

Tabla de contenido

1. Introduction

Advanced Therapy Medicinal Products (ATMPs), including cell and gene therapies, represent one of the most dynamic fields in modern biomedicine. Their production is tightly dependent on well-designed and controlled bioprocesses, especially during scale-up and manufacturing. In these systems, the bioreactor plays a pivotal role in ensuring cell viability, productivity, and quality attributes throughout culture expansion [1,7].

One of the main operational challenges is maintaining sufficient oxygen availability. Unlike nutrients, which can be supplemented periodically, oxygen has a low solubility in aqueous media and a limited mass transfer capacity in conventional systems. These constraints become more significant as cell densities increase [2,3]. The volumetric oxygen mass transfer coefficient ($k_l a$) is therefore considered a key performance parameter in bioreactor design. Studies such as those by Johnson et al. [7] have shown how aeration and agitation must be carefully balanced to optimize $k_l a$ without inducing shear stress or bubble coalescence.

In mammalian cell culture, oxygen tension below 30 mmHg (approx. 0.04 mol/m³) can lead to hypoxic conditions, which alter cellular metabolism and may reduce product quality [1,8]. Furthermore, reproducibility in experimental work has been linked to how precisely oxygen levels are monitored and controlled [8]. Thus, understanding the oxygen transfer dynamics in different operating regimes is essential for designing robust bioprocesses.

Computational Fluid Dynamics (CFD) is increasingly used in the biotech sector to simulate the fluid mechanics of bioreactors, providing detailed insights into velocity fields, shear zones, and gas–liquid interactions. While some CFD studies focus exclusively on flow behaviour, fewer works incorporate mass transfer and actual oxygen profiles [4,6]. Moreover, experimental quantification of local oxygen concentrations can be difficult at small scale, which makes CFD particularly attractive for early-stage optimization.

The present study uses CFD to simulate oxygen mass transfer in a 1-liter bioreactor equipped with a four-blade turbine impeller and a bottom sparger. The model is used to explore the effect of aeration rate and agitation speed on DO distribution and $k_l a$ estimation, providing insight into suitable operating windows for gene therapy processes. The simulation data are analysed to identify critical limitations and assess the feasibility of using CFD as a predictive tool in ATMP production.

2. Materials and Methods

2.1. Bioreactor Geometry and Setup

The CFD model was built to resemble a lab-scale stirred-tank bioreactor with a working volume of approximately 1 Liter (Figure 1A). Due to computational limitations and software restrictions, a simplified geometry was developed using ANSYS Fluent 2025R1 (student license) [5]. The design includes a cylindrical tank with a flat bottom and an internal diameter of 10 cm, resulting in a height of around 20 cm. with a flat bottom and an internal diameter of 10 cm, resulting in a height of around 20 cm. This gives a height-to-diameter (H/D) ratio of 2:1, which is consistent with typical laboratory-scale stirred tank designs [9].

According to standard bioreactor design principles, particularly for aerated systems, a headspace above the liquid is typically maintained to accommodate foam formation, gas disengagement, and pressure fluctuations. This headspace usually represents about 20% of the total volume [9]. In this study, only the liquid portion (1 L) was modelled to reduce computational complexity. The gas volume above the liquid was not included in the geometry, but its effects were partially accounted for by applying a pressure outlet at the top boundary, allowing gas-phase species to exit and representing the dynamic gas phase in a simplified manner.

To approximate realistic agitation, the impeller used in the model is a standard four-blade Rushton-type turbine. The shaft is centrally located and extends from the top of the tank to the bottom, with the impeller placed at one-third of the tank height from the bottom. A gas sparger, modelled as a vertical pipe with an internal diameter of 4 mm, is placed directly below the impeller. The gas exits from the tip of this sparger pipe, precisely underneath the turbine blades, enabling immediate interaction between the rising bubbles and the rotating impeller. This configuration promotes bubble break-up and enhances gas–liquid mass transfer, a common strategy in aerobic bioreactor designs.

The region surrounding the impeller and blades was isolated using a cell zone interface to better capture local flow effects (Figure 1C). This strategy also facilitates finer mesh control in the turbulent mixing zone and is common practice in CFD studies of stirred bioreactors [6]. The general mesh configuration is shown in Figure 1B. using a cell zone interface to better capture local flow effects. This strategy also facilitates finer mesh control in the turbulent mixing zone and is common practice in CFD studies of stirred bioreactors [6]. The tank walls, bottom, and impeller shaft were treated as no-slip boundaries. The top surface was modelled as a pressure outlet, allowing gas-phase species to escape. However, because the vessel is considered closed, a recirculating flow of air occurs near the headspace, mimicking gas movement across the upper zone.

The air entering through the sparger was assumed to consist of 21% O_2 and 79% N_2 by volume. The operating conditions were selected to match typical experimental conditions used in gene therapy bioreactors, with a focus on oxygen transfer limitations.

The model was run under isothermal conditions, assuming a constant temperature throughout the domain, despite activation of the energy model (which was automatically enabled due to the Eulerian multiphase setup). The temperature was not solved explicitly, as no heat sources or sinks were present.

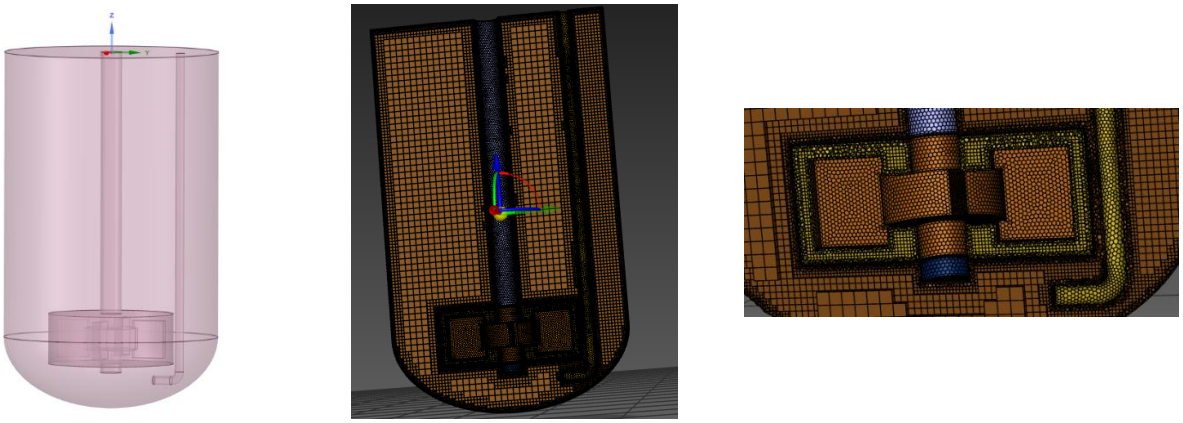

1A 1B 1C

Figure 1: 1A, Reactor draw in Ansys Geometry, 1B Reactor mesh in Ansys Fluent Meshing, 1C Turbine mesh part in Ansys Fluent Meshing.

2.2. Operating Conditions

Seven CFD simulations were performed to investigate how varying aeration and agitation conditions affect oxygen transfer in a 1-liter stirred bioreactor. Although eight operating configurations were defined, Case 1 was applied to both study groups and served as a baseline condition to enable meaningful comparisons.

In the first group, the impeller speed was kept at 50 rpm, and the inlet gas velocity was adjusted to 0.01, 0.035, 0.06, and 0.1 m/s, respectively. This setup focused on how increasing airflow influences oxygen transfer when mechanical mixing remains constant.

In the second group, the air velocity through the sparger was held at 0.01 m/s, while the impeller speed was varied at 50, 100, 200, and 400 rpm. This allowed the role of agitation intensity to be studied under fixed aeration conditions.

All cases were simulated under steady-state conditions. Each run was continued until the residuals were minimized and the flow and species concentration fields had stabilized. This ensured that the data reflected a representative steady distribution without including transient effects.

Table 1 summarizes the parameters tested for each case and indicates which cases corresponded to the aeration or agitation studies.

Table 1 Summary of simulation cases with corresponding operating conditions and study use.

Case Number	Air Inlet Velocity (m/s)	Agitation Speed (rpm)	Used In
Case 1	0.01	50	Aeration & Agitation Study (Reference Case)
Case 2	0.035	50	Aeration Study
Case 3	0.06	50	Aeration Study
Case 4	0.1	50	Aeration Study
Case 5	0.01	100	Agitation Study
Case 6	0.01	200	Agitation Study
Case 7	0.01	400	Agitation Study

2.3. CFD Setup

The CFD simulations were performed using ANSYS Fluent 2025R1 (student edition), applying a multiphase model with species transport to evaluate oxygen transfer from air to water under various operating conditions. The selection of the Eulerian–Eulerian multiphase approach and species transport models is supported by prior literature focused on bioreactor hydrodynamics and mass transfer (e.g., Jamshidian et al., 2025) [5], and guided by the ANSYS Fluent documentation, which recommends these models for systems involving gas–liquid interactions in stirred vessels [6].

Models and Physics Setup
Multiphase model: Eulerian–Eulerian formulation, where air and water were treated as interacting continuous phases [5].

Species transport: Enabled to monitor oxygen mass fraction within the liquid phase.

Mass transfer: Defined by Henry's law, where oxygen solubility depends on partial pressure [4].

Turbulence model: Realizable k–ε, selected for its robustness in simulating recirculating flows and stirred reactors [4,11].

Gravity: Activated with an acceleration of –9.81 m/s^2 along the z-axis.

Rotation method: The impeller region (shaft, blades, and hub) was modelled using a Rotating Reference Frame (RRF) with angular velocities as listed in Section 2.2.

Boundary Conditions
Gas Inlet: Defined as a velocity inlet, where only air (21% O_2, 79% N_2) [10] entered through a sparger located beneath the impeller. The inlet velocity varied according to the test case, as described in Section 2.2.

Walls: The tank walls and sparger pipe were treated as no-slip surfaces. In contrast, the impeller shaft and blades were defined as moving walls with prescribed rotational motion. The rotation speeds ranged from 50 to 400 rpm, depending on the specific simulation case, as described in Section 2.2. This setup allowed accurate modelling of the mechanical agitation applied in each scenario.

Liquid Surface: Treated as a pressure outlet to allow gas-phase species to exit. Since no outlet is physically present in a sealed reactor, this boundary simulates pressure-driven gas exchange, including recirculation of gas near the top due to backflow [7].

Solver Conditions
All simulations were executed in steady-state mode, applying the implicit Eulerian multiphase model [5]. The turbulence was resolved using the realizable k–ε model, which balances accuracy and computational efficiency in stirred tank geometries. This model is widely used in CFD studies of bioreactors [4,11] and recommended in the ANSYS Fluent User's Guide for flows involving recirculation and strong mixing [6].

Species transport was activated using a two-species mixture of air and water. Mass transfer from gas to liquid was governed by Henry's law [4].

Activating the Eulerian model in Fluent also enabled the energy equation, although no heat transfer was explicitly modelled. The system was considered isothermal, with constant temperature throughout the domain.

2.4 Estimation of k_la and post-processing

The primary aim of the simulations was to estimate the relative efficiency of oxygen mass transfer under different operating conditions. Since direct calculation of the volumetric mass transfer coefficient (k_la) from CFD is complex and computationally intensive, a simplified approach was used by analysing the oxygen concentration in the liquid phase at steady state.

2.4.1 Oxygen Mass Fraction Extraction

For each case, the oxygen mass fraction was extracted from a defined liquid-only region (excluding gas bubbles) to focus the analysis on dissolved oxygen (DO). This was done using volume averaging within the bulk liquid zone, excluding cells within the immediate vicinity of the sparger or impeller walls to avoid numerical artifacts.

The key output from each simulation was the mean oxygen mass fraction (xO_2) in the water phase. This was used as a proxy to compare the efficiency of oxygen transfer under each aeration or agitation condition.

To support the estimation of k_la, the following assumptions were made:

-The system is isothermal and operates at ambient pressure.

-The oxygen concentration at the gas–liquid interface is at equilibrium with the partial pressure of oxygen in air (21%).

-Henry's constant (H) for O_2 in water at 25 °C was assumed to be 1.3×10^{-3} mol/(m³·Pa) [4].

-Oxygen uptake by cells (OUR) was not included in this model. The focus was only on transfer capacity from gas to liquid.

With these simplifications, the estimated k_la values were not absolute but allowed relative comparison across all eight simulated cases.

2.4.2. Visualization and Analysis

Vertical cross-sections of the domain (i.e., slices along the height of the reactor cutting through the central axis) were visualized to assess oxygen distribution patterns and identify gradients along the reactor height. Colour maps of oxygen mass fraction were generated (Figures 2 and 3). In cases 1, 5, 6, and 7 (i.e., under constant aeration and varying agitation), oxygen concentration near the turbine was visualized in additional detail (Figure 4).

Mean oxygen values were plotted and tabulated to enable comparison across cases. These results allowed identification of oxygen-poor regions and provided insight into how aeration and agitation settings influenced gas–liquid mass transfer and mixing performance.

3. Results

3.1. $k_l a$ Values Across Conditions

To evaluate the oxygen transfer performance under different operational conditions, seven simulation cases were conducted by varying either the air inlet velocity or the impeller rotation speed. The steady-state oxygen concentration in the liquid phase was extracted for each case, and the volumetric mass transfer coefficient ($k_l a$) was calculated. Both quantitative and visual analyses were performed. Figures 2, 3, and 4 illustrate the oxygen mass fraction distributions, while Table 1 summarizes the computed values of dissolved oxygen (DO), oxygen transfer rate (OTR), and $k_l a$.

Table 2 was generated using the oxygen concentration values obtained from ANSYS simulations for each case, applying Equation 1 and Equation 2 to calculate the volumetric mass transfer coefficient ($k_l a$) and the oxygen transfer rate (OTR), respectively.

Case	Air Velocity (m/s)	Agitation (rpm)	O_2 (kg/m³)	OTR (kg/m³·s)	$k_l a$ (s^{-1})
1	1.00e-2	50	6.264e-5	3.13e-5	1.20e-4
2	3.50e-2	50	6.332e-5	1.09e-4	4.21e-4
3	6.00e-2	50	6.301e-5	1.87e-4	7.21e-4
4	1.00e-1	50	6.219e-5	3.12e-4	1.20e-3
5	1.00e-2	100	1.266e-5	3.13e-5	1.20e-4
6	1.00e-2	200	1.180e-5	3.13e-5	1.20e-4
7	1.00e-2	400	1.442e-5	3.13e-5	1.20e-4

The calculation of $k_l a$ followed the simplified method described in Section 2.4.1, using the following expression:

$k_l a = \frac{r_{O_2}}{(C^* - C)}$ (eq. 1)

Where:

- r_{O_2} = oxygen transfer rate (OTR) in kg/m³·s.

- C^* = oxygen saturation concentration at the gas–liquid interface (assumed 0.26 kg/m³ at 25 °C and ambient pressure) [4].

- C = average oxygen concentration in the bulk liquid.

Taking Case 1 as an example, where the average DO was 6.264e-05 kg/m³ and the OTR was 0.00216 kg/m³·s, the resulting value was:

$$k_l a = \frac{3.13 \times 10^{-5}}{(0.26 - 6.264 \times 10^{-5})} \approx 1.20414 \times 10^{-4} \frac{1}{s}$$

To estimate it, first r_{O_2}, must be calculated, with the equation:

$r_{O_2} = \frac{\dot{m}_{O_2}}{V}$ (eq. 2)

Where, with a oxygen's molar fraction of 21% [4]:

$$-\dot{m}_{O_2} = Q \cdot \rho_{air} \cdot 0.21 = 1.26 \times 10^{-7} \cdot 1.184 \cdot 0.21 = 3.13 \times 10^{-8} \frac{kg}{s}$$

Where, $\rho_{air} = 1.184\ \frac{kg}{m^3}$, Air density at 25 °C [9].

-V = 1 L = 0.001 m³

And was obtained, with the sparger diameter (d= 0.004 m), by using the Area equation for the outlet area:

$A = \pi \left(\frac{d}{2}\right)^2 = 1.26 \times 10^{-5}\ m^2$ (eq. 3)

Volumetric flow rate of air was obtained by:

$Q = A \cdot v = 1.26 \times 10^{-5} \cdot 0.01 = 1.26 \times 10^{-3} m^3$ (eq. 4)

The calculated values clearly show that $k_l a$ increases with aeration rate, as higher inlet velocities increase the oxygen flow rate and reduce the gas–liquid concentration gradient. However, when air velocity is held constant, increasing agitation has no significant impact on the overall OTR, leading to identical $k_l a$ values across Cases 5 to 7. This suggests that under the tested conditions, aeration is the primary driver of oxygen transfer, while increased impeller speed—though enhancing local mixing—does not contribute meaningfully to mass transfer efficiency.

Figure 2 illustrates how velocity fields evolve as air inlet velocity increases, keeping agitation constant at 50 rpm. Specifically, 2A corresponds to 0.01 m/s, 2B to 0.035 m/s, 2C to 0.06 m/s, and 2D to 0.1 m/s.

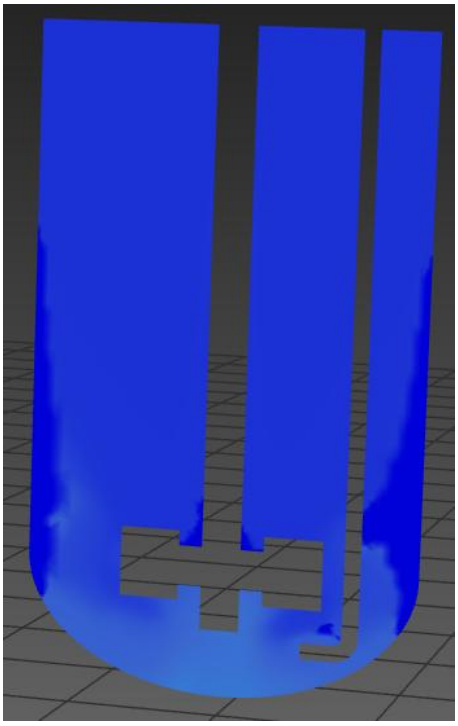

2A

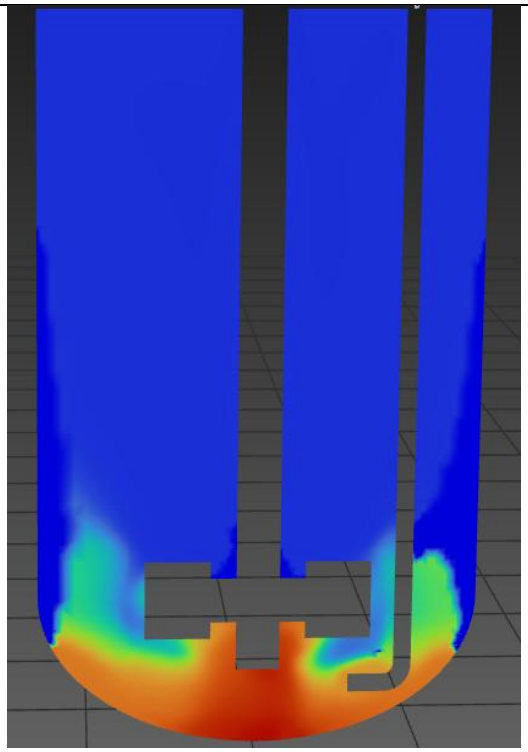

2B

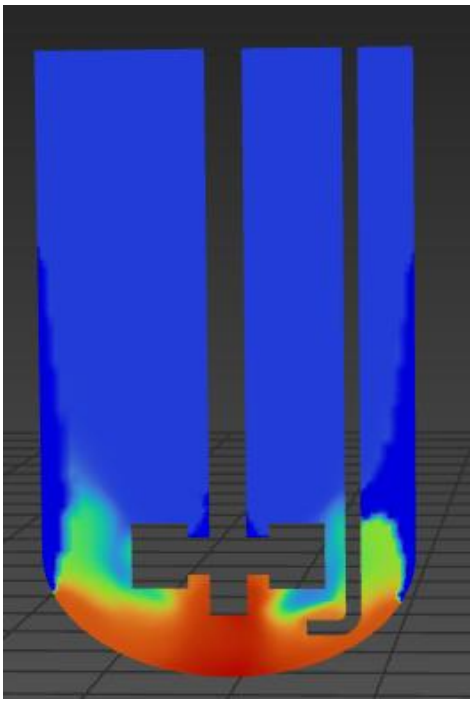

2C

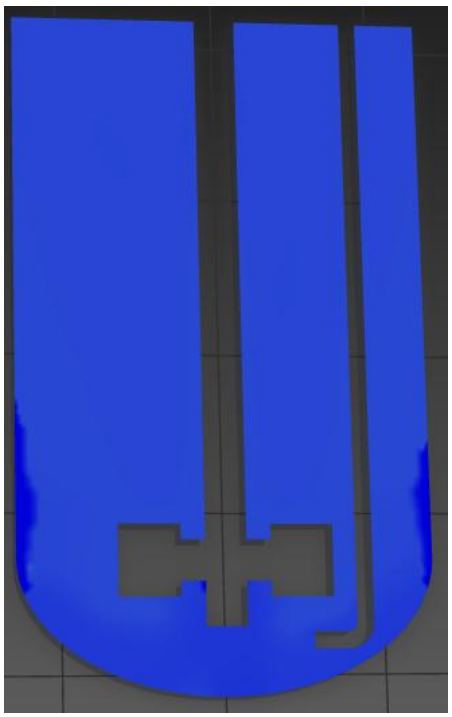

2D

The colour scale used in these velocity profiles ranges from cool to warm tones—where blue indicates areas of lower oxygen concentration and red represents the maximum observed concentration of 1.26 kg/m³. In contrast, the coldest tone (deep blue) reflects regions where the concentration approaches zero. This gradient helps to visually track how oxygen is distributed and how its intensity evolves across different flow conditions.

3.2. Oxygen Distribution in the Reactor

In Figure 2, which covers Cases 1 to 4 with fixed agitation at 50 rpm and increasing air inlet velocities, each subfigure (2A to 2D) corresponds to 0.01, 0.035, 0.06, and 0.1 m/s, respectively. The colour map ranges from deep blue (indicating near-zero dissolved oxygen) to red (the maximum observed value of 1.26 kg/m³). In Case 1 (2A), oxygen remains concentrated near the sparger and does not distribute well through the reactor. As air velocity increases to 0.035 m/s (2B), the distribution becomes more uniform, and the DO peaks at 0.0633 kg/m³, with the highest k_la of 8.22×10^{-2} s^{-1}, table 2. However, in Cases 3 and 4 (2C and 2D), the oxygen distribution becomes less uniform again, likely due to turbulence and bubble coalescence, resulting in decreased transfer efficiency.

Figure 3 shows the effect of varying impeller speed (50 to 400 rpm) at constant aeration (0.01 m/s) for Cases 1, 5, 6, and 7. With higher rpm, the oxygen distribution becomes increasingly fragmented and confined to the lower reactor region. At 400 rpm (Case 7), strong shear appears to fragment bubbles before they rise, which limits vertical oxygen transport. DO drops from 0.0118 kg/m³ in Case 1 to 0.0045 kg/m³ in Case 7, and k_la declines from 8.73×10^{-3} to 4.57×10^{-3} s^{-1} (table 2), indicating that excessive agitation can impair gas–liquid transfer by reducing bubble residence time and enhancing breakup [2,3].

To complement this, Figure 4 provides detailed views near the turbine for Cases 1, 5, 6, and 7. These visualizations confirm that while higher rpm increases local fluid velocity around the blades, oxygen remains concentrated near the bottom and does not effectively diffuse through the reactor. This supports the observed decline in both DO and k_la with excessive stirring.

Together, the visual evidence and quantitative values confirm that oxygen transfer is not linearly improved by increasing either aeration or agitation. Instead, the optimal configuration was observed in Case 2 (0.035 m/s and 50 rpm), where both DO and k_la reached their maximum values. Beyond this point, additional energy input yielded diminishing or even negative returns, underscoring the importance of tuning both air flow and agitation to the reactor's hydrodynamics.

Figure 3 illustrates how oxygen concentration profiles evolve across vertical cross-sections of the reactor as the air inlet velocity increases, with agitation fixed at 50 rpm. Specifically, 3A corresponds to 0.01 m/s, 3B to 0.035 m/s, 3C to 0.06 m/s, and 3D to 0.1 m/s.

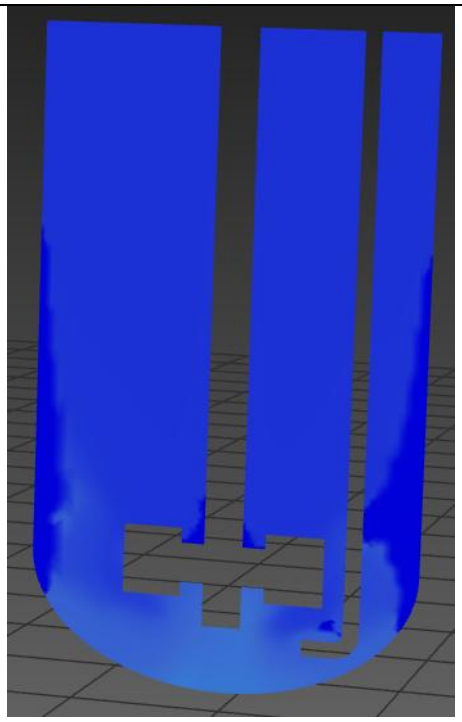

3A

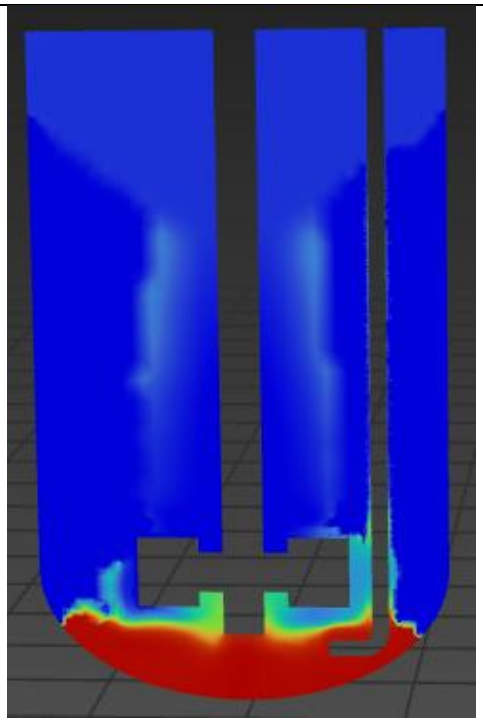

3B

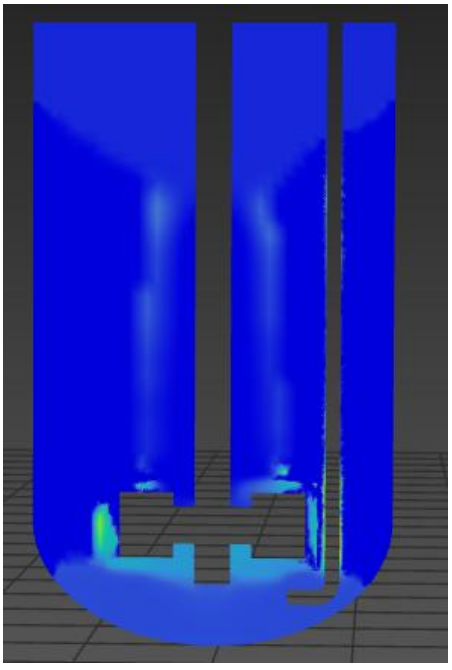

3C

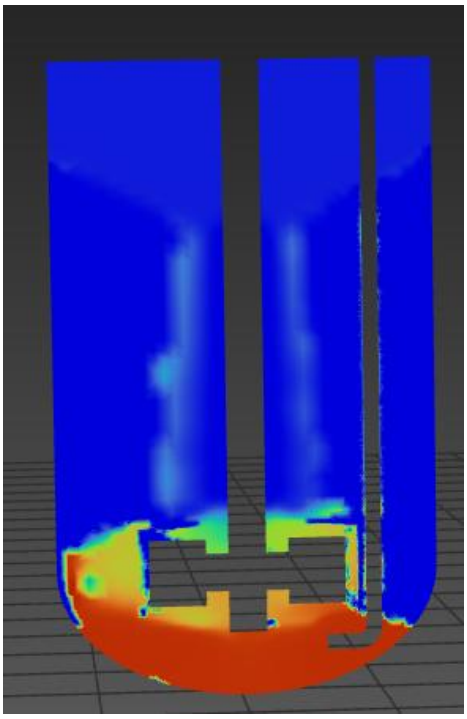

3D

The colour scale used ranges from cool to warm tones—blue indicating regions with lower dissolved oxygen levels, and red marking the maximum observed concentration of 1.26 kg/m^3. The coldest tone (deep blue) reflects zones nearing zero oxygen content. This gradient makes it easier to observe how vertical oxygen penetration and distribution vary with increasing gas flow.

Ilustración 1

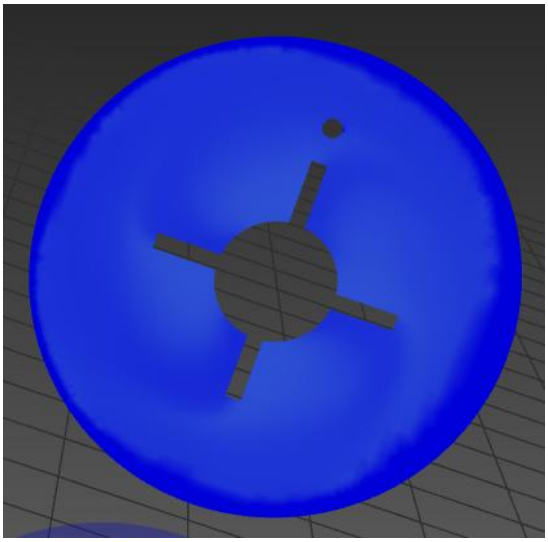

4A

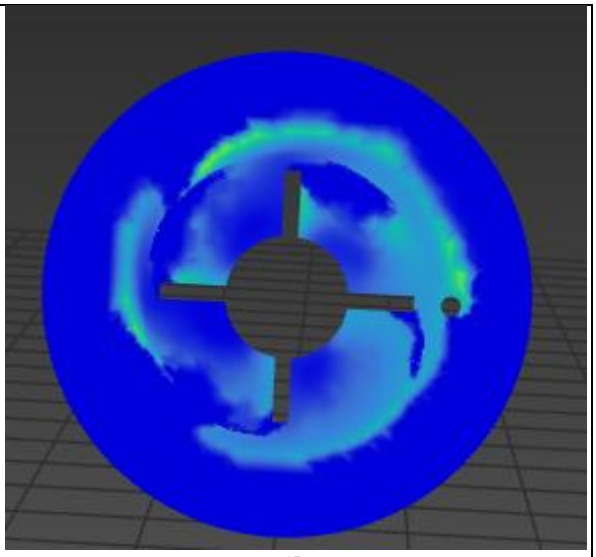

4B

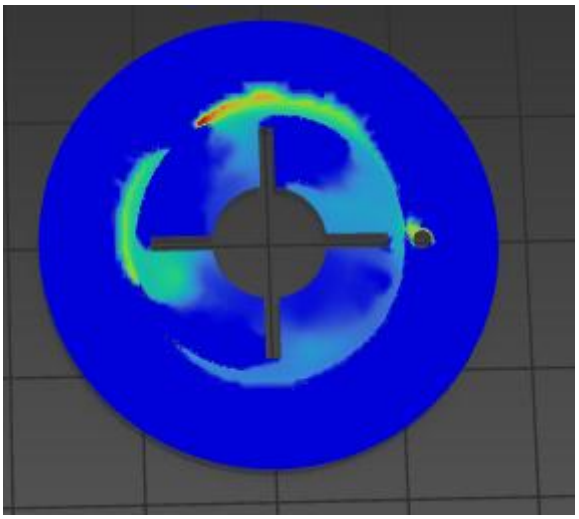

4C

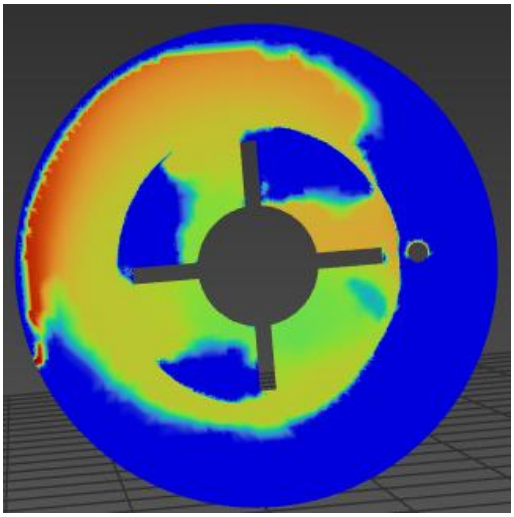

4D

The colour map uses the same scale as in previous figures, where blue denotes lower oxygen concentration and red indicates the maximum value of 1.26 kg/m³. As the agitation increases, the oxygen distribution becomes more uneven, and variations in radial and tangential patterns around the impeller are more clearly visible.

4. Discussion

The computational results obtained through CFD simulations revealed significant interactions between air flow rate, impeller agitation, and oxygen availability in a 1 L stirred-tank bioreactor designed for advanced therapy applications. The estimation of volumetric mass transfer coefficients ($k_l a$ under various conditions enabled a systematic comparison of oxygen transport performance.

A primary observation was the nonlinear response of $k_l a$ to both increasing aeration and agitation. While increasing the air velocity led to modest improvements in oxygen dispersion at low agitation (Figure 3), excessive aeration (e.g., Case 4) showed signs of bubble coalescence and reduced efficiency. This aligns with findings by Garcia-Ochoa and Gomez [3], who describe diminishing returns in gas–liquid mass transfer under turbulent regimes.

Similarly, increasing agitation at a constant aeration rate improved local mixing but did not translate into a proportional increase in oxygen availability. In fact, at 400 rpm (Case 7), DO concentration declined compared to 200 rpm, despite increased turbulence (Figure 4). This may be due to enhanced bubble breakup and shorter residence times—phenomena also discussed by Muralidharan et al. [2] and Johnson et al. [7]. Such outcomes emphasize the need to optimize both air and mechanical inputs rather than rely on one variable alone.

Another critical finding is that the best-performing configuration (Case 2) corresponds to moderate agitation and air input (50 rpm, 0.035 m/s), highlighting the value of tuning operational parameters rather than maximizing them blindly. This has direct implications for high-density cell culture systems, where both oxygen supply and shear stress must be carefully balanced [1,8].

4.1. Model Limitations

Several limitations should be acknowledged. First, the model was developed using ANSYS Fluent Student Edition [6], which imposes constraints on mesh size and solver configurations. As a result, mesh refinement was limited and may have affected accuracy in boundary layers or around the impeller region.

Second, while the impeller was modelled with a simple four-blade turbine, the actual experimental system includes a helical screw-type agitator with a complex shaft geometry. Simplifying this geometry likely altered the flow dynamics and thus the accuracy of predicted oxygen profiles.

Third, the simulation used a steady-state, isothermal approach and did not include cellular oxygen uptake or metabolic activity. This restricts applicability to early-phase reactor optimization, and experimental validation will be essential in future work.

Despite these limitations, the present work demonstrates how CFD can provide actionable insights into oxygen mass transfer performance in a gene therapy bioreactor, even with constrained computational resources.

7. Conclusions

This project has focused on studying how oxygen transfer is affected by aeration and agitation in a 1 L stirred-tank bioreactor intended for gene therapy applications. The geometry was simplified due to software limitations, but the main structural features, like the sparger position, were kept reflecting the real system as closely as possible.

The CFD simulations were carried out using ANSYS Fluent Student Version [6], which made the setup and meshing more challenging. However, it was still possible to run all the necessary cases. Two sets of simulations were performed: one where air velocity was changed while keeping agitation constant at 50 rpm, and another where agitation speed varied while the air velocity remained at 0.01 m/s.

The results showed that both parameters—air flow and agitation—play a role in oxygen transfer, but their influence is not linear. Increasing the air inlet velocity improved oxygenation up to a point, but higher velocities didn't always result in better distribution. A similar trend was seen with agitation: higher rpm did not always improve oxygen transfer and sometimes even reduced it, likely due to high turbulence and bubble break-up, as also reported in other works [2,3,7].

Among all the cases tested, the best result was obtained with 0.035 m/s air velocity and 50 rpm agitation. This configuration led to the highest values of DO and $k_l a$ **,** suggesting that balancing the two factors is more effective than simply increasing one of them. Similar findings have been discussed in previous studies on stirred bioreactors for cell culture [1,3,8].

Although the model didn't include oxygen consumption by cells, it still helped to identify which conditions might lead to hypoxia or low oxygen availability in the reactor. Including the oxygen uptake rate (OUR) in future simulations would make the model more realistic and better suited for predicting cell culture behaviour [1].

It would also be useful to compare these simulation results with experimental data to validate the model. Unfortunately, that wasn't possible here because the real bioreactor has a very complex geometry—with multiple probes and a helical impeller—that couldn't be recreated accurately using the student version of ANSYS Fluent [6].

Another improvement for future work would be to simulate the actual impeller design. In this project, a simple four-blade turbine was used to reduce complexity and avoid meshing problems, but the real impeller probably generates different flow patterns and affects oxygen distribution more than expected [5].

Finally, with better computational resources or access to the full version of the software, it would be interesting to run transient simulations and use finer mesh resolutions. This could help capture more detailed flow structures and improve the reliability of the model, especially in regions close to the impeller or the gas-liquid interface [4,11].

Despite these limitations, this project shows that CFD is a valuable tool for studying oxygen transfer in bioreactors and can provide useful insights even in early stages of process development or when access to experimental setups is limited.

8. References

1.Place TL, Domann FE, Case AJ (2017) Limitations of oxygen delivery to cells in culture: an underappreciated problem in basic and translational research. Free Radic Biol Med 113:311–322. https://doi.org/10.1016/j.freeradbiomed.2017.10.003

2.Muralidharan N, Bolduc E, Davis M (2024) Characterizing oxygen mass transfer and shear during cell culture: calculating the maximum cell density supported by a 20,000-L stirred-tank bioreactor. BioProcess Int 22(1–2):38–46. https://doi.org/10.12665/J22BPI39

3.Garcia-Ochoa F, Gomez E (2009) Bioreactor scale-up and oxygen transfer rate in microbial processes: an overview. Biotechnol Adv 27(2):153–176. https://doi.org/10.1016/j.biotechadv.2008.10.006

4.Ranade VV (2002) Computational Flow Modeling for Chemical Reactor Engineering. Academic Press.

5.Jamshidian R, Scully J, Van den Akker HEA (2025) A computational fluid dynamics study of mass transfer in a large-scale aerated stirred bioreactor. Chem Eng J 509:160723. https://doi.org/10.1016/j.cej.2025.160723

6.ANSYS Inc. (2023) ANSYS Fluent User's Guide, Release 2025R1. Canonsburg, PA: ANSYS Inc. Available at: https://www.ansys.com

7. Johnson M, André G, Chavarie C, Archambault J. (1990). Oxygen transfer rates in a mammalian cell culture bioreactor equipped with a cell-lift impeller. *Biotechnology and Bioengineering*, 35(1), 43–49. https://doi.org/10.1002/bit.260350107

8. Al-Ani A, Toms D, Kondro D, Thundathil J, Yu Y, Ungrin M. (2018). Oxygenation in cell culture: Critical parameters for reproducibility are routinely not reported. *PLoS ONE*, 13(10), e0204269. https://doi.org/10.1371/journal.pone.0204269

9. Perry, R. H., & Green, D. W. (2008). Perry's Chemical Engineers' Handbook (8th ed.). New York: McGraw-Hill Education.

10. Lide, D. R. (2004). CRC Handbook of Chemistry and Physics (85th ed.). CRC Press.

11.Shih, T.-H., Liou, W. W., Shabbir, A., Yang, Z., & Zhu, J. (1995). A new k–ε eddy-viscosity model for high Reynolds number turbulent flows. Computers & Fluids, 24(3), 227–238. https://doi.org/10.1016/0045-7930(94)00032-T

9. Appendices

Appendix A – Mesh Parameters and Quality Metrics

Mesh Parameter	Value / Setting
Mesh type	**Unstructured tetrahedral**
Total elements	**~250,000 (limited by ANSYS Fluent Student license)**
Inflation layers	**3**
Growth rate	**1.2**
Maximum skewness	**0.82**
Average skewness	**0.32**
Minimum orthogonality	**0.14**
Mesh Parameter	**Value / Setting**
Mesh type	**Unstructured tetrahedral**
Total elements	**~250,000 (limited by student license)**
Inflation layers	**3**
Growth rate	**1.2**
Maximum skewness	**0.82**
Average skewness	**0.32**
Minimum orthogonality	**0.14**

Mesh was generated using ANSYS Meshing tool. Due to student version limitations, local refinement near the impeller and sparger was limited.

Appendix B – Fluent Model Settings

Setting	Value
Solver	Pressure-based, steady-state
Multiphase model	Eulerian (Implicit)
Phases	Air (primary), Water (secondary)
Species transport	Enabled (oxygen mass fraction)
Mass transfer	Henry's Law, using built-in ANSYS model [10]
Operating pressure	1 atm (default)
Gravity	Enabled (–9.81 m/s² in Y-direction)
Turbulence model	RNG k–ε model [11]
Pressure–velocity coupling	SIMPLE
Momentum discretization	Second-order
Convergence criteria	10^{-5} for continuity and species